Vigilada Mineducación

DIGITAL PLATFORM APPROACH FOR HYDRAULIC CHARACTERIZATION AND DETECTION OF HYDRODYNAMIC PHENOMENA IN REVERSIBLE TURBOMACHINES.

DAVID ALEJANDRO MEJÍA OCAMPO.

Tipo de trabajo (Tesis)

Asesor, docente
Francisco Javier Botero Herrera.

UNIVERSIDAD EAFIT
ESCUELA DE INGENIERÍAS
MAESTRÍA EN INGENIERÍA

Digital platform approach for hydraulic characterization and detection of hydrodynamic phenomena in reversible turbomachines

David Alejandro Mejía Ocampo [a].

[a] *Escuela de ingeniería, Universidad EAFIT, Colombia.* dmejiao2@eafit.edu.co

Abstract

Hydroelectric power is one of the most developed and used renewable energy sources in terms of installed capacity and reliability; therefore, it is one of the electricity production methods with the highest contribution worldwide and with an important level of technological maturity. In recent years, the hydropower sector is moving from large to small power plants, due to the limitations of water resources and the effects of climate change. In addition, reversible hydraulic turbomachines, although less used, are postulated as alternatives to offset the demand for intermittent renewable energy technologies that are difficult to forecast. This article presents the development and implementation of a digital platform based on real-time measurements for monitoring, recording, and analysis in the time and frequency domains of hydromechanical, dynamic, and electrical quantities. The resulting data are suitable for the characterization of the hydraulic machines, and their technical diagnosis, allowing the detection of complex phenomena that may occur during their operation. To illustrate some of the capabilities of the platform, experimental tests were carried out on a specific low-speed centrifugal pump, through its four-quadrant characteristic curve. The focus was on measuring pressure fluctuation and acceleration (vibrations) during operation at its best efficiency point (BEP) and at one off-design operating point where hydrodynamic instabilities were detected. Finally, analysis and results are exposed, and the characteristics are presented.

Keywords: Digital platform; Four-quadrant curve; Hydrodynamic phenomena; Pressure fluctuations; Pump as Turbine (PaT); Reversible turbomachine.

Nomenclature

$\tilde{a}_{1,2}$	Accelerations (vibrations) [m/s^2]	Z	Position [m]
D	Impeller diameter [m]	**Greek letters**	
E	Specific hydraulic energy [J/kg]	η	Efficiency [%]
f	Characteristic frequency [Hz]	ϕ_i	Keyphasor [-]
f_s	Sample rate [kS/s]	ρ_w	Water Density [kg/m^3]
f_n	Pressure fluctuation frequency [-]	θ_w	Water temperature [°C]
H	Hydraulic head [m]		
H_s	Setting level [m]	**Subscripts**	
NPSH	Net positive suction head [m]	BEP	Best Efficiency Point
$n_{1,2,3}$	Impeller rotational speed [rpm]	BPF	Blade Passage Frequency
n_{ED}	Speed factor [-]	FS	Full Scale
N_{QE}	Specific Speed [-]	IDAS	Integrated Data Acquisition System
P	Power [W]	OP	Operation Point
$P_{1,2}$	Static pressure [kPa]	MHP	Micro Hydro Power Plant
$\tilde{p}_{1,2}$	Pressure fluctuation [Pa]	PaT	Pump as Turbine
Q	Discharge flow rate [m^3/s]	PHES	Pumped Hydro Energy Storage
Q_{ED}	Discharge factor [-]	SHP	Small Hydropower Plant
T	Shaft torque [N.m]	SSF	Signal switching frequency
T_{ED}	Torque factor [-]	TSA	Time Synchronous Average

1. Introduction

1.1 Generalities and Applications

Hydropower is one of the most developed and widely used renewable energy sources in terms of installed capacity and reliability; therefore, it is one of the clean electricity production methods with the highest contribution worldwide and an important level of technological maturity. The flexibility of hydropower allows it to seamlessly integrate other energy sources and act as a force multiplier for other renewables and makes it an invaluable resource for feeding into the grid after a blackout. There are three types of hydroelectric facilities: impoundment, diversion, and pumped storage [1].

In recent years, the hydropower sector is moving from large to small power plants, due to the limitations of water resources and the effects of climate change. Therefore, given the growing demand for energy (electricity), its high price, and the need to access clean renewable energies [2], reversible hydraulic turbomachines, although less used, are postulated as alternatives to offset the demand for intermittent renewable energy technologies or those that are difficult energy forecasting [3], such as wind, solar, tidal, and among other power generation solutions that are at the center of the energy transition towards a more sustainable and reliable electricity source model.

Reversible hydraulic turbomachines have been adapted to market needs to operate in Small-scale hydropower plants and pumped hydro energy storage (PHES) micro facilities. The most widely accepted categories worldwide are micro [4] and small [5] hydropower plants.

A micro hydropower plant (MHP) has a capacity of up to 100 kilowatts, while small hydropower plants (SHP) have a capacity of between 100 kilowatts and 10 MW [1]. These plants are usually of the "run-of-the-river" type, which means that they do not require the use of a reservoir, i.e., only a small dam is created so that pipes divert part of the flow, let it fall a slope, and pass through the turbomachine, spinning it, which in turn activates the rotor of a generator to produce electricity [6]. This is how these small power plants convert the potential energy of streams and watercourses into kinetic energy to produce electricity, providing economical and reliable power generation without too high an environmental impact.

On the other hand, PHES works like a giant battery and can be integrated into a smart grid and store electricity generated by other energy sources, such as solar, wind, nuclear, and others, for later use. These facilities store energy by pumping water from a lower reservoir to an upper reservoir to support the stability and security of the electrical grid [7]. Another advantage of these projects is that they can be integrated with the local power grid and can operate day and night and in all weather conditions if there is a constant flow of water, to ensure the security of power supply under uncertain operating conditions or during periods of peak electricity demand.

Therefore, especially a Pump Operating as a Turbine (PaT) is postulated worldwide as a successful solution to offset the demand for clean renewable energy technologies in small-scale hydroelectric projects [8]. Centrifugal pumps are reversible hydraulic machines that, depending on the direction of rotation of the impeller can operate as pumps or as turbines, allowing to change the direction of flow quickly and being able to operate under off-design operating conditions without any structural modification.

In addition, these machines have a lower price than hydraulic turbines, as they are mass-manufactured and available in standard sizes. However, few software options on the market are adaptable, flexible, modular, portable, and capable of working with the different types of sensors

needed to perform the complete hydraulic performance test [9], characterize it, and study its hydrodynamic phenomena, under different operating regimes and off-design conditions.

Usually design laboratory facilities or specialized software for experimental testing of models and research dedicated exclusively to pumps or turbines [10], [11] according to the design specifications of the machines. Nevertheless, despite the great versatility of PaTs in the market, it is not easy to correctly define their performance since the characteristic curves in turbine mode are not provided by the pump manufacturers. In fact, there is a lack of information from the suppliers of this type of machines, as well as a lack of technological platforms that allow an efficient and effective evaluation to characterize the hydrodynamic phenomena that can occur in these machines.

Several studies have indicated that these machines can have many fields of application. For instance, such as generation alternatives for rural electrification [12], [13] in remote locations with difficult access and energy deficiencies, energy recovery in water systems[14], [15], replacement of pressure-reducing valves (PRVs) in Water Distribution Networks (WDN) [16], [17], micro energy storage and smart water grids [18], among other applications.

On the other hand, some research has presented methods for the selection of PaTs in micro-hydroelectric power plant applications [19], methodologies for the prediction of their performance curves, and numerical methods to predict the best efficiency point (BEP) [20]. In addition, in recent years, computational fluid dynamics (CFD) has become a vital methodology for investigating the performance of PaTs [21].

Nevertheless, despite the many advantages of using these machines, it has been observed that their operation is associated with the occurrence of different hydraulic instability phenomena, characterized by pressure fluctuations [22] and vibrations. It has been mentioned that these hydraulic instabilities can cause loss of efficiency, a premature mechanical failure of the machine, or even an unplanned shutdown. Therefore, many of the recent studies have focused more on the flow stability aspects of hydraulic turbomachines, where pressure and acceleration fluctuations within the machine have been the research focus [23].

A convenient way to characterize all the operating modes of a turbomachine is through the four-quadrant curve proposed by Knapp in 1937 [24], which relates the rotational speed and discharge under all possible conditions of flow, head, and speed in any direction. The fact that these machines can rotate and deliver flow in two opposite directions gives them the operating characteristics of the so-called "four quadrants", allowing them to operate in five defined regimes, namely: turbine, turbine-brake, pump, pump-brake, and reverse pump.

The characteristics and working conditions of each regime were presented by Amblard et al. [25]. Thus, the characterization of a turbomachine with the four-quadrant curve allows us to know the behavior in all its operating modes and to identify those areas where hydrodynamic phenomena may occur [26]. Figure 1 shows the four-quadrant characteristic curves available in the technical literature. Dimensionless terms for discharge factor, speed factor, torque factor, and power factor (Q_{ED}, n_{ED}, T_{ED} and P_{ED}) have been used in this article, according to the equations established in the IEC-60193 [27] standard of the International Electrotechnical Commission.

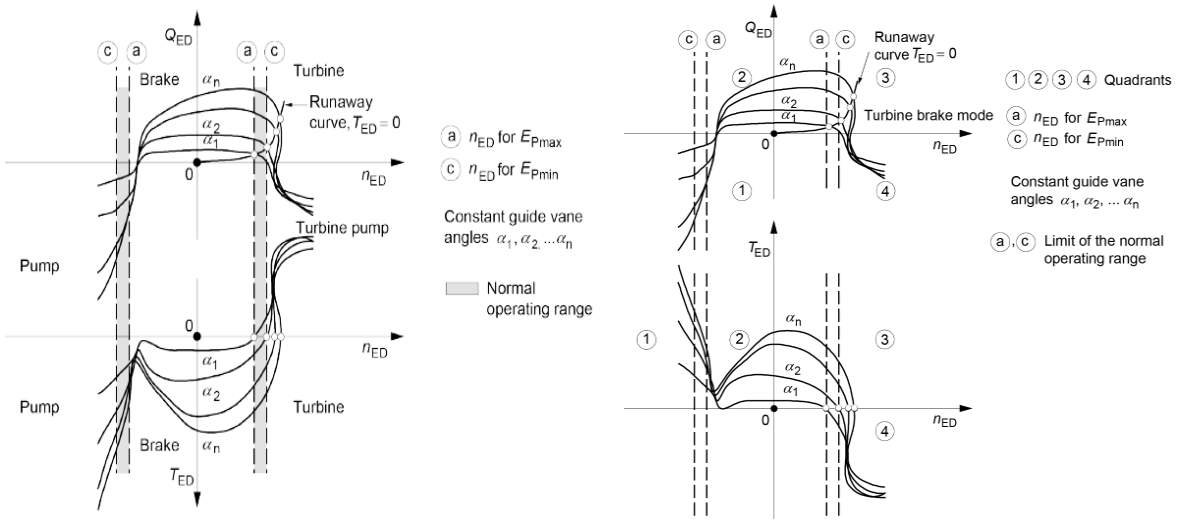

Figure 1. General four-quadrant diagram of a reversible turbomachine, showing the modes of operation as a function of impeller diameter **D**, specific hydraulic energy **E**, flow rate ***Q***, and rotational speed ***n***. Data and curves are from reference [27]

This paper presents the development of a new digital platform that aids the detailed characterization of reversible hydraulic turbomachines, especially PaTs for small-scale power generation. Since centrifugal pumps coupled to an induction motor are often commercialized, the necessary elements for the simultaneous study of the electric machine have also been considered. For the design of the platform, it was considered that these hydraulic and electric machines will be operating in conditions even opposite to those of their original design. This translates into enormous challenges to properly acquire, manipulate, process, and visualize data to detect and evaluate complex phenomena.

Therefore, the platform is conditioned to handle both stochastic and deterministic variables, hydraulic, mechanical, and electrical in nature, i.e., they are examined in the time, frequency, and time-frequency domains. The TDMS format was adopted to provide the platform with the ability to easily exchange information with other information processing systems and thus avoid the costly and time-consuming design and maintenance of architectures and databases. The result is binary files, efficiently structured for high-speed writing [28].

Along with the description of the platform, an experimental case study is introduced, which makes it possible to illustrate the operation of the platform, highlight its main resources and qualitatively expose the technical diagnostics of some typical phenomena of these machines. Although it is focused on a small PaT, the methodology is extensible to larger-scale power generation and even different types of turbomachines.

First, a sweep of the entire operating range is made as a reversible turbomachine to build the characteristic curves. Then, the results of five notable operating points are selected and compared. For example, synchronous hydrodynamic fluctuations are measured and compared, such as those induced by the passage of the turbomachine impeller blades, and asynchronous ones such as low-frequency recirculation. Mechanical vibrations of the casing and the power supply of the electrical machine are also analyzed.

The detection of hydrodynamic phenomena and their analysis was carried out according to the methods indicated in other previously published investigations [11], [29]-[30]. The detailed study of the behavior of the machine throughout all its characteristics offers relevant technical information, for one hand to establish policies on the operating ranges that maximize the efficiency and the remaining useful life (RUL) of the turbomachinery, and on the other hand, to reveal, avoid and mitigate undesirable phenomena.

When turbomachines operate under off-design conditions, their efficiency decreases, and different hydraulic phenomena appear to endanger the stability of the machine, especially when operating in deep part load, part load, high part load, and full load regime [31], reducing the lifetime of the components and, therefore, increasing the operating and maintenance costs. However, these phenomena do not always occur in the same way. For the case of the four-quadrant characteristic curve, different hydraulic phenomena occur depending on the operating regimes each of them of a different nature.

Cavitation, turbulence, Rotating Stall (RS), Rotor Stator Interaction (RSI) [32], and vortex rope are some of the hydraulic phenomena that often occur. For that reason, as a first step, it is necessary to study how, and which phenomena can be detected with the different sensors. For the study, a total of 12 sensors were installed, and distributed in the hydraulic circuit and the turbomachine under study. Nevertheless, the focus has been on the measurement of pressure fluctuation and vibrations during operation at its BEP and at two off-design operating points where hydrodynamic instabilities have been detected. The main dominant hydraulic phenomenon occurring close to the BEP is the RSI [31].

The hydraulic phenomena affecting the performance of a turbomachine are numerous and very complex. For this purpose, Brennen [33] presented a classification system consisting of three different categories of flow oscillations. Such as, (A) Global flow oscillations, (B) Local flow oscillations, and (C) Radial and rotodynamic forces. Thus, it indicated at least 12 existing hydrodynamic phenomena, related to radial and rotodynamic shaft forces, sub-synchronous unsteady flows associated with flow recirculation at the inlet of a centrifugal impeller, and other unsteady drawbacks encountered in turbomachines, including their oscillation frequencies.

In addition, some research has focused on the study of these phenomena. Hasmatuchi et al. [34] experimentally investigated the pressure fluctuations and the occurrence of RS in a turbine-pump under off-design operating conditions. Botero et al. [35] have presented non-invasive measurement methods for the measurement of sub-synchronous phenomena attributed to RS, especially at the operating points related to the S-shaped characteristic curve in the pump-turbine. Also, Bolaños et al. [26] presented the four-quadrant characterization of a low specific speed centrifugal pump, to characterize a turbomachine, to know the behavior in all its operating modes, and to identify those operating zones where hydrodynamic phenomena may occur. However, in many cases, visualization of hydrodynamic phenomena is not possible and external indications, such as noise and vibrations, are not enough to clearly identify them. Consequently, it is very important to make available new digital platforms based on real-time measurements to assist the detailed characterization and technical diagnosis of reversible turbomachines.

2. Materials and Methods

This section will present the illustrative setup of the experimental case study, a brief introduction of the parameters of the reversible turbomachine, together with the details of the digital platform, instruments, and experimental procedures. The methodology implemented for the development of the digital platform was carried out in three stages. In the first stage, experimental tests were carried out for the real-time characterization of the turbomachine, through its four-quadrant curve. In the second stage, stable and unstable zones and operating points were identified, to measure and detect dynamic fluctuations associated with possible hydrodynamic phenomena.

Finally, with the database recorded during the experimental tests and using computational tools, graphs were developed to identify possible phenomena. For this purpose, time, and frequency domain analysis methods, such as Time Synchronized Averaging (TSA) and power spectra, were used to

present the spectral components related to the hydrodynamic oscillations induced by the Blade Passage Frequency (BPF) of the turbomachine under study, as a function of the hydrodynamic instabilities and the operating conditions.

2.1 Hydraulic System

The experimental tests were developed on a specific low-speed centrifugal pump, through its four-quadrant characteristic curve, in a test rig developed at the Hydraulics Laboratory of the EAFIT University, for the study of reversible hydraulic turbomachines, according to the installation requirements for model acceptance tests established in the IEC 60193 [27] standard. This system is equipped with two commercial centrifugal pumps, both manufactured in 316 stainless steel by ITT-Gould's pumps [36] series SSH. In this article, the term "Turbomachine under study" refers to a specific centrifugal pump (Model 5SH).

This machine is connected in series with an electro-pneumatic flow control valve, to a closed-loop hydraulic piping circuit fed by water from an open storage tank, whose volume of 2.5 m^3 is larger than the volume of the closed-loop to ensure that the entire piping system always remains pressurized, providing sufficient submergence of the turbomachine under study and restricting the entry or displacement of air bubbles. Besides this, the energy to move water within the circuit is supplied by the drive of a recirculation pump (Model 8SH) which can deliver a maximum discharge of 0.0119 m^3/s and a maximum pressure head of 18 meters water column (mWC) respectively. Thus, the way of directing the flow within the circuit allows simulating different hydraulic load levels and various hydraulic conditions, either to operate a turbomachine as a pump or PaT. The diagram in Figure 2 illustrates the test rig schematic with its most important components.

On the other hand, the test rig has a system of rubber flexible hoses with quick coupling and acrylic tubes that allow observing hydrodynamic phenomena and flow patterns at the inlet and outlet of the machine (high- and low-pressure reference sections).

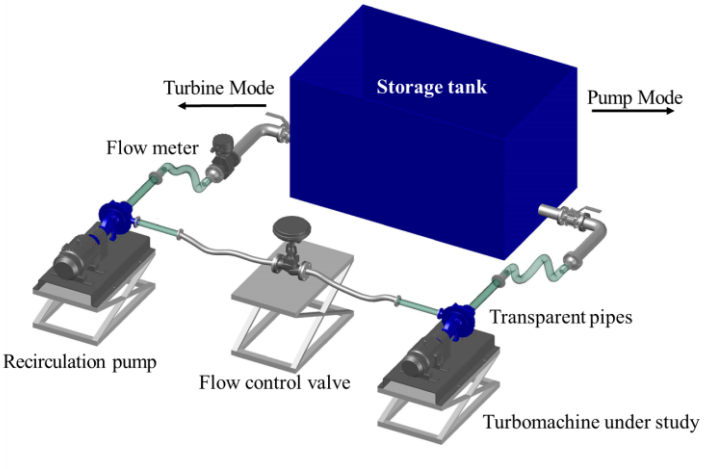

Figure 2. Schematic diagram of the hydraulic test rig.

The hydraulic characterization of the turbomachine under study and the measurements of its hydrodynamic phenomena were carried out through its four-quadrant curve, using the dimensionless terms indicated in IEC 60193 [27]. The measurements made during the experimental test were carried out by adjusting the test rig with a set level lower than 10 mWC.

In addition, to achieve the variation of the test head, speed factor, and discharge factor, an automatic control system acting on the electro-pneumatic valve, the rotational speed of the study turbomachine, and the recirculation pump were implemented.

2.2 Mechanical and Electrical System

The turbomachine under study on which the measurements and analyses were carried out has a power capacity of 2.0 HP and a closed channel impeller with 6 blades. The main technical characteristics are summarized in Table 1. The recirculation pump has a power capacity of 3.0 HP, both units have a nominal diameter suction of 0.0635 m and a discharge nominal diameter of 0.0508 m. The test rig power system was implemented with a 208VAC/60Hz three-phase power supply, distributed in two circuits. The first 208VA line-to-line circuit powers the variable frequency drives (VFDs) that drive the electric motors. The second 120VAC line-to-neutral circuit feeds a single-phase uninterruptible power supply (UPS), which supplies regulated power to the computer, as well as to the DC-24VDC power supplies required by the measurement instruments and control equipment.

Table 1. Main technical characteristics of the hydraulic and electric machine.

Turbomachine	Design features	Motor	Nameplate
Impeller Inlet diameter	0.08104 [m]	Enclosure US Motors	NEMA Premium Efficiency
Impeller outlet diameter	0.14764 [m]	Power	2.0 [HP]
Number of impeller blades – backswept	6 [un]	Wound stator and rotor	60Hz/4 pole/1745 [rpm]
Rated rotor speed	1750 [rpm]	Electrical power input	Three-phase 208 [V]
Flow rate	0.009 [m^3/s]	Load current	5.6 [A]
Dynamic head	10 [mWC]	Max reactive power	1.2 [kVAr]
Mechanical power	1491.4 [W]	Slip	3.05 [%]
Specific Speed	0.11 [-]	Torque	10.9 [N.m]
Efficiency	65 [%]	Efficiency	86.5 [%]

The entire measurement system consists of sensors, transmitters, an interconnection system of cables and connectors, and intelligent controllers that manage the digital platform operation. Besides, the selected motor is a three-phase, low-voltage, squirrel-cage, Class B induction motor designed for variable torque loads, including centrifugal pumps. The motor provides a starting torque of 150% of rated torque at full load and operates with no more than 5% slip at rated load, according to the National Electrical Manufacturers Association (NEMA) [37].

2.3 Integrated Digital Platform

For the development of the processing structure, a distributed architecture with two properly configured and synchronized signal acquisition and processing systems was adopted. The master National Instruments® CompactRio® cRIO-9045 [38] controller contains the modules for the acquisition and conditioning of the hydromechanical and dynamic signals and the control actions. The second controller or slave cRIO-9076 [38] contains the modules for the acquisition and conditioning of the electrical power signals. The capacity, flexibility, and reliability of these electronic devices, combined with the performance of Field Programmable Gate Array (FPGA) modules, allowed the researchers at EAFIT University to develop a digital platform based on real-time measurements, called TurboLogger software in the LabView® environment.

This digital platform was developed to integrate the functions of measurement, data acquisition, and real-time monitoring of deterministic and stochastic signals with high sampling rates and high resolution, thus ensuring continuous and multichannel measurement. Furthermore, its functionalities allowed the development of an easily adaptable, flexible, modular, portable, safe, and innovative program, able to work with different types of sensors, whose processing structure was specialized and designed for the characterization of reversible hydraulic turbomachines and the study of their hydrodynamic phenomena. The process blocks implemented in the software development and testing phases are shown in Figure 3.

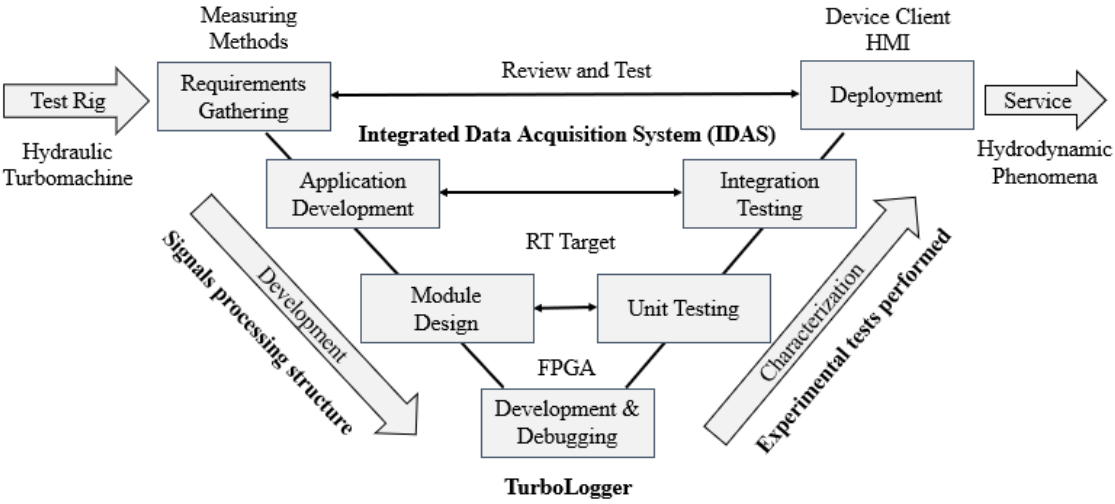

Figure 3. Integrated process blocks for measurement and processing of the digital platform.

It should be noted that the digital platform was developed to integrate the processes of measurement, acquisition, and continuous processing of hydrodynamic, dynamic, and electrical power signals; also includes real-time calculation of parameter results for machine characterization. As well as the visualization of the magnitudes represented by the test measurements and the storage of the data in the cloud. Additionally, it was designed to provide real-time measurement tools for the detection and analysis of some hydrodynamic phenomena. Its implemented structure of dedicated loops allowed to improve system performance by reducing network traffic, controlling, and monitoring data flow.

Based on this, it is guaranteed that during the various information transfer and storage processes, overflows, and underflows, i.e., data or record losses, did not happen. In addition to the above, its integrated data acquisition system (IDAS) has been designed to be portable, modular, and scalable so that it can manage and operate a wide variety of measurement equipment depending on the different hydrodynamic phenomena of interest. The position of the dynamic sensors the turbomachine under study, as well as the main controller of the digital platform, can be seen in Figure 4.

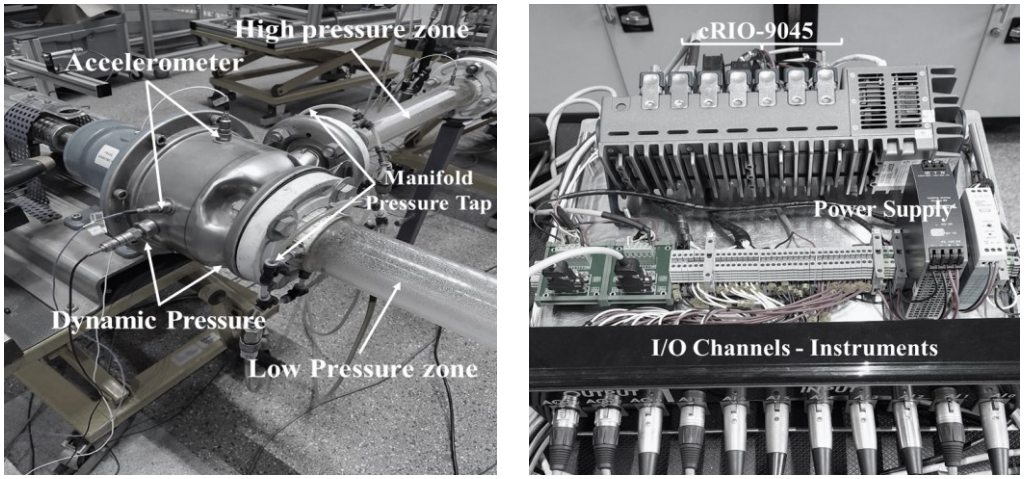

(**a**) (**b**)

Figure 4. (a) Dynamic sensors installed on the turbomachine, (b) Main controller of the digital platform.

One of the main advantages of the digital platform methodology is to provide a Common Data Environment (CDE), which allows all researchers to work from the same program model while ensuring that

everyone is using the most upgraded version of the software, the basic configuration parameters, and the same database. Considering that everyone is working with the same updated model, there are no unintentional conflicts due to using an outdated version, it also makes scope changes much easier to manage and implement, as the impact of any change is immediately available to all parties, analysts, and researchers. In this way, the platform environment was a central data record for all the documentation of the research project, facilitating the management of the large volume of information generated during the experimental tests. The storage and connectivity of the database in the CDE allowed the development of collaborative work between the analyst and the researchers during the different phases of the tests and the post-processing of the data.

Finally, another important aspect of the digital platform was the Ethernet TCP/IP communication network architecture that was implemented between the controllers, the workstation, the remote client, the laboratory's wireless communication network, and the management of dedicated cloud storage of the digitized data. This approach allows data to be centralized, stored, and shared securely during all stages of research.

2.4 Measuring Equipment

The test rig is equipped with several measuring instruments to record all the test conditions and to process the deterministic signals involved during the exploration of the four quadrant characteristics, such as static pressure, rated head, discharge, rotor speed, torque, shaft power, energy content, efficiency, and electrical power signals. In addition, it has high-resolution, and accuracy sensors that guarantee the reliability of the frequency response produced by vibrations, as well as a high sampling rate to record the pressure fluctuations that occur within the turbomachine. This type of equipment is essential to properly sample the signals produced by the complex phenomena that appear in turbomachines in off-design operating conditions, according to the IEC 60193 standard [27]. Figure 5 shows the experimental setup of the test rig.

Therefore, deterministic, and stochastic signals were classified into four groups as follows: **Group (a)** for all hydromechanical signals used for machine characterization. **Group (b)** exclusively for dynamic signals used to study hydrodynamic phenomena. **Group (c)** integrates the electrical power signals used to analyze the phenomena produced by power supply fluctuations, and **Group (d)** is assigned to the control signals. This classification allowed the specific selection of the hardware components and the development of the software processing structure. Six acquisition modules [39] and a series of measuring instruments have been selected that fit the classification of the four groups. The general technical characteristics of the equipment used are described lines below.

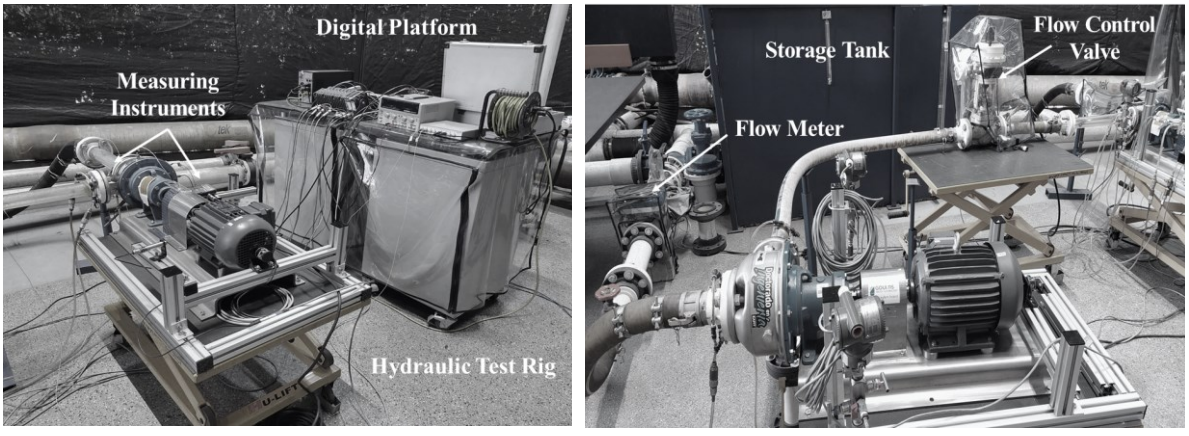

(**a**) (**b**)

Figure 5. (a) Turbomachine under Study, (b) Location of the components of the hydraulic test rig and recirculation pump

To record the stochastic hydromechanical signals, an NI 9203 module and the following instruments were connected. Three pressure transmitters were used to measure the static pressure and the differential between the inlet and outlet $\mathbf{P_{1,2}}$ reference sections of the machine (upstream and downstream). They were fitted at the same reference level **Z** at the pressure taps (piezometric ring), which is possible since the turbomachine is positioned horizontally.

In addition, a bidirectional electromagnetic flowmeter was used to measure the discharge flow rate $\boldsymbol{Q}$ and a PT100 transducer is used to record the water temperature $\boldsymbol{\theta_w}$. These electronic devices were installed in the high-pressure zone of the closed loop, between the storage tank and the recirculation pump. Such instruments are required to calculate quantities such as the specific hydraulic energy **E** (or hydraulic head **H**), the suction-specific potential energy $\mathbf{E_s}$ (or the setting level $\mathbf{H_s}$), and net positive suction energy **NPSE** (or its corresponding **NPSH**), among others. All signals assigned to the NI 9203 module are conditioned, buffered (multiplexed), and sampled by a single 16-bit Delta-Sigma (ADC) at a rate of 200 kS/s, i.e., the channels were sequentially scanned several times over a given period, fast enough so that no data is lost. Besides, a NI 9401 high-speed module was also installed to measure the rotational speed $\boldsymbol{n_{1,2}}$, phase $\boldsymbol{\phi_i}$ and direction of rotation. TTL signals from a three-phase encoder are buffered with a maximum signal switching frequency of up to 30 MHz.

To record the dynamic signals, three NI 9232 modules and the following measuring instruments were installed: Two piezoelectric pressure transducers (DYT1 and DYT2) to measure pressure fluctuations $\widetilde{\boldsymbol{p}}_{\mathbf{1,2}}$, positioned in the casing, both located at an offset angle of 45° apart, with sensitivity to detect dynamic phenomena in frequency ranges from 1 Hz to 40 kHz. Two accelerometers (AC1 and AC2) for measuring vibrations $\widetilde{\boldsymbol{a}}_{\mathbf{1,2}}$ installed on the casing surface, both with an offset angle of 90° apart, designed for vibration analysis on rotating machinery, with a frequency response of 0.5 to 10 kHz.

Finally, a dynamic torque transducer has been installed to record to measure the shaft torque **T**. All inputs of the NI 9232 modules are conditioned and then sampled by 24-bit isolated ADCs with simultaneous sampling architecture between channels (synchronized) at a rate of 102.4 kS/s/Ch, which allowed investigation of hydrodynamic phenomena up to 102.4 kHz. Such modules are fitted with real-time digital filters implemented in hardware to prevent aliasing. All dynamic sensors are integrated piezoelectric electronic sensors (IEPE) of high sensitivity, isolated from GND for noise immunity. Besides, their input channels are BNC to avoid electromagnetic interference (EMI) and protected against surges. The main technical characteristics of the measuring instruments, controllers, and modules used, are given in Table 2.

An optical digital tachometer and a torque transducer have been installed to record the keyphasor signal $\boldsymbol{\phi_i}$ and measure the shaft torque fluctuations **T** of the turbomachine shaft. It should be noted that these instruments were grouped with dynamic signals, and the tachometer was adapted to generate a TTL volts signal. All inputs of the NI 9232 modules are conditioned and then sampled by 24-bit isolated ADCs with simultaneous sampling architecture between channels (synchronized) at a rate of 102.4 kS/s/Ch, which allowed investigation of hydrodynamic phenomena up to 51.2 kHz. Such modules are fitted with real-time digital filters implemented in hardware to prevent aliasing.

To record the electrical power signals, NI 9246 and NI 9225 modules were installed: These two modules were used to measure the current $\mathbf{I_{1,2,3}}$, voltage $\mathbf{V_{1,2,3}}$ applied or generated at the motor terminals. Active power, apparent power, reactive power, phase angle displacement (power factor), phase sequence, frequency, and harmonics can be estimated from these signals. All input channels are surge protected and conditioned and sampled by 24-bit ADCs. Because of the above, all signals were collected simultaneously (synchronized) at a rate of 50 kS/s/Ch, which allows the investigation of phenomena associated with electrical power up to 25 kHz. Finally, an NI 9265 module was used to control the test rig, using analog current output signals (4 to 20 mA) assigned by the test rig operator and PID controllers, thus executing the rotational speed and flow

control actions. These parameters are essential to execute and simulated different control strategies (speed, torque, and flow rate), including the start-up sequence and synchronization processes with the grid in turbine mode [40].

Table 2. Main characteristics of measuring instruments and controllers.

Instruments	**Output**	**Range**	**Span**	**Linearity**	**Sensitivity**
PT - Yokogawa-EJA530E	4...20 [mA]	0...2 [bar]	2bar	±0.055 [%FS]	-
Flow meter Khrone-IFC100	4...20 [mA]	0...0.033 [m^3/s]	0.033 [m^3/s]	±0.25 [%FS]	-
GE TransPort PT878	4...20 [mA]	0...0.033 [m^3/s]	0.033 [m^3/s]	±0.25 [%FS]	-
PT100 Wika TR30-W	4...20 [mA]	-50...250 [°C]	300 [°C]	±1 [%FS]	-
Optical Tachometer DT2234C+	TTL 0...5 [V] pulse	2.5...99996.5 [rpm]	99994 [rpm]	0.05 [%] +1 digit	0.1 [rpm]-2.5…999.9 [rpm] 1[rpm] over1000[rpm]
Encoder Omron E6B2-C-CWZ3E	TTL 0...5 [V] pulse	0…6000 [rpm]	6000 [rpm]		-
Rotary Torque Futek-TRS600	±5 [V]	-20...20 [N.m]	40 [N.m]	±0.2 [%FS]	-
Dynamic pressure Dytran-2005V	0...5 [V]	0...50 [psi]	50 [psi]	±1 [%FS]	100 [mV/psi]
Accelerometer Dytran-3055D6T	±5 [V]	±25 [m/s^2]	50 [m/s^2]	±1 [%FS]	198 [mV/g]
Controllers	**Module**	**Characteristics**	**Resolution**	**Sample rate**	**Signals**
cRIO-9045 – Chassis 8 slots FPGA: Kintex-7 7K70T Number of flip-flops: 82.000 Number of DSP: 240 Number of DMA channels: 16	NI 9203	Al 8-Ch 0 to 20 [mA]	24-Bit	200 [kS/s] (Multiplexed)	(**a**) Hydromechanical
	NI 9401	8 DIO, 5 [V/TTL]	-	SSF 30MHz (Multiplexed)	
	NI 9232	Al 3-Ch ±30 [V]	24-Bit	102.4 [kS/s] (Simultaneous)	(**b**) Dynamic
	NI 9265	AO4-Ch 0 to 20 [mA]	16-Bit	100 [kS/s] (Simultaneous)	(**c**) Control
cRIO-9076 – Chassis 4 slots FPGA: Xilinx Spartan-6 LX45 Number of lip-flops: 54.576 Number of DSP: 58 Number of DMA channels: 5	NI 9246	AI 3-Ch ±20 [Arms]	24-Bit	50 [kS/s] (Simultaneous)	(**d**) Electric power
	NI 9225	AI 3-Ch ±300 [Vrms]	24-Bit	50 [kS/s] (Simultaneous)	

The instrumentation used was verified following the guidelines of the equipment assurance program established by the metrology and hydraulics laboratory of EAFIT University. The laboratory's quality management system establishes the procedures to ensure the correct operation of the measuring equipment, the quality of the achieved results, and the accuracy required for the test execution. This ensures that the errors associated with the measurements are within the range defined by the instrument manufacturer and the recommendations established by IEC 60193 [27]. The above guidelines ensured a level of confidence greater than 95% in the measurement results presented in this article. Nevertheless, to avoid random errors and systematic errors, during some tests similar instruments were installed in parallel to carry out simultaneous verification readings.

2.5 Software Processing Structure

Hydraulic, mechanical, and electrical quantities are acquired and conditioned by specialized modules. Some variables are dynamic in nature, such as mechanical vibrations, pressure fluctuations, and electrical variables. In this case, anti-alias filters, AC coupling, determinism, and synchronization are important. Other variables, such as flow rate and static pressures, are stochastic in nature, so their acquisition is less demanding. The phase and angular velocity of the machine shaft are obtained from pulse trains produced by encoders. A high-speed digital module is used for this purpose. The control of the angular speed of the machines and the opening of the flow control valve is achieved from analog current signals.

All samples acquired by the different modules are centralized and processed in a Field Programmable Gate Array (FPGA). It executes deterministic cycles in parallel at high data-to-clock rates appropriate for

each module and uses high-speed direct memory access (DMA) channels to exchange information with the real-time controllers (cRIO-9045 and cRIO9076). The controllers execute the most complex mathematical operations (floating point), sorting the information, and making it available to the client (PC-Client).

This last function is achieved by implementing a high-performance TCP/IP network based on NI's Shared Variables Engine (SVE) technology [41]. The SVEs are executed within each cRIO and use the NI Publish-Subscribe Protocol (NI-PSP) to enable the transfer of shared variable data over a network. For each quantity group, a specific reading or writing variable was assigned, dedicated exclusively to making available to each controller or client the most recent data collected during the test. As shown in Figure 6, the information flow of each quantity group is distinguished using different colors. In green, the dynamic variables, in blue, the hydrodynamic variables of stochastic behavior. Finally, in red, the variables related to electrical power signals.

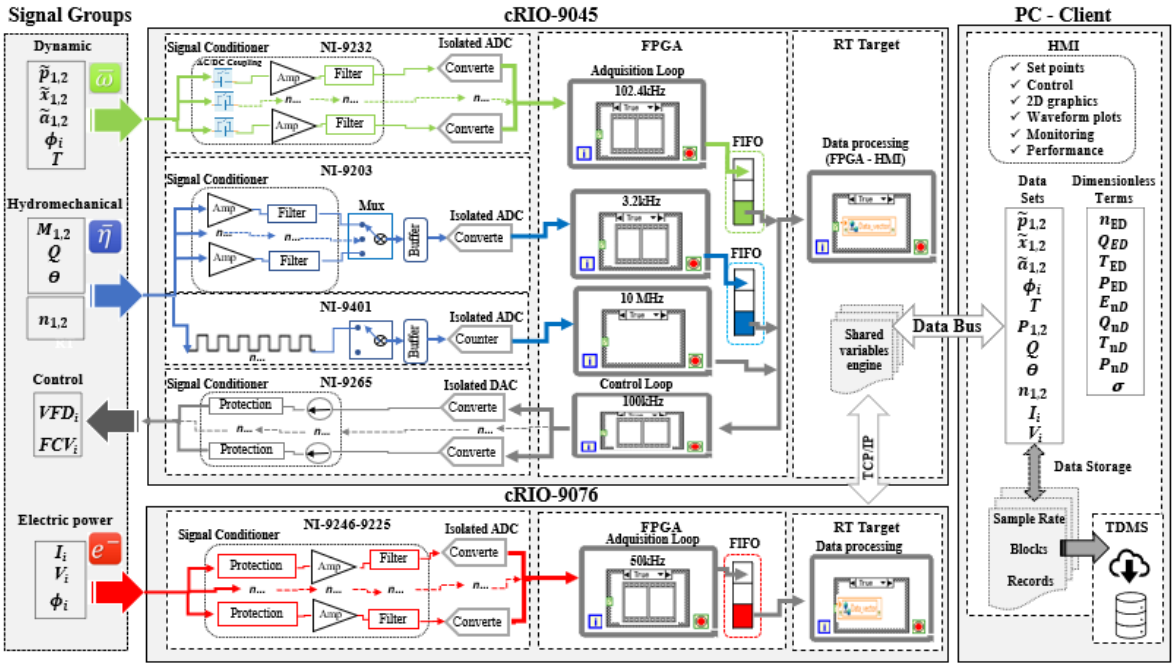

Figure 6. Diagram of processes and data communication paths of the digital platform.

As mentioned earlier, data transfer operations were carried out through DMA channels. This is a method based on the First In First Out (FIFO) table that is used to transfer large amounts of data at high speeds between the FPGA and the RT Target application, i.e. the cRIO controllers, ensuring that the FPGA I/O nodes do not overflow due to the high number of samples per channel.

The interconnection is fully managed by variables published on the network. This approach, therefore, allows data to be centralized, stored, and shared securely at all processing stages, ensuring synchronized communication between the controllers and the client. Figure 6 shows the grouping of the mentioned quantities and the modules used for signal acquisition and conditioning of each group. It also includes the signal acquisition and conditioning processes, filtering, multiplexing, buffering, analog-to-digital conversion (ADC), and data acquisition and control loops.

In addition, the structure developed in terms of software allowed the integration of data acquisition processes, communication between controllers, measurement analysis, monitoring, and automatic control for real-time visualization of performance parameters and analysis in the time and frequency domains of the hydromechanical, dynamic and electrical quantities of the turbomachinery.

As well as the storage and processing of big volumes of data. It was decided to use the TDMS (Technical Data Management Streaming) format native to NI, to save the information in a systematic and structured way. This format was developed to optimize the high-speed transmission of large volumes of structured data. Those are TurboLogger's technical requirements due to the complex logistics of the expected tests. Another important aspect that was considered when selecting the TDMS format was its availability to be used in other widely used work programming environments, such as MATLAB® and Python software, an especially appreciated attribute in the post-processing stages.

Finally, the project is based on a three-tier structure in which software applications of different levels are responsible for the assigned tasks and run on their corresponding hardware targets: The first-level application is the high-level interface with the client, the human-machine interface (HMI), dedicated to communication with the operator or analyst of the test rig. It performs tasks such as setting control parameters, editing configuration values, monitoring the sensors, and managing performance tests. This module runs on the PC-Client.

The second-level application manages real-time communications for data processing and exchange, actuation, and drive and control signals for the electro-pneumatic flow control valve, recirculation pump, and turbomachine under study, using proportional-integrated-derivative (PID) algorithms. This module runs on each of the controllers (RT Target), in real-time on each controller at the CPU level. The third level application is delegated to the scan interface and is responsible for storing and processing the data from each of the NI C series I/O modules, i.e., this application performs the processes of reading the input channels and writing the output channels. It runs on the (FPGA) embedded chip.

3. Results and Discussion

3.1 The Human-Machine Interface (HMI)

The PC-Client application is designed to be executed from a computer and is developed in a conventional three-step sequence model (initialization, processing, and events). The first step is Initialization, this process includes the initialization functions of the system variables; the data arrays; and the preparation of the 2D plots of the hydromechanical, dynamic, electrical, and control signals. It also includes TSA, polar and 3D waterfall plots to analyze the spectral components of each Operating Point (OP) of interest. In addition, during the shutdown, the output channels related to the control signals are set to a safety default value. Figure 7. Shows a mosaic with different screens of the HMI. It presents the development of the different windows, where some results and plots of the raw data recorded during experimental tests can be observed.

The second step includes the functions to read signals from the input channels, perform basic conditioning of statistical data (such as mean, standard deviation (σ), and median) and write to the output channels. In addition, this process includes three main while loops that are started sequentially: The first while loop executes the measurement processes of the stochastic and deterministic variables, as mentioned above, intended for the machine characterization tasks and the study of hydrodynamic phenomena; The second while loop executes the measurement processes of the electrical power variables, to analyze the power system; The third while loop is dedicated to the control actions.

The third step includes the sequence of events, this structure is mainly used to configure the reading channels assigned to each of the inputs of the NI modules, set the sampling frequency, assign the number of samples per channel, and adjust the control parameters of the test rig. In addition, it is used to monitor communication between the controllers. It also includes options to enable or disable readout channels, instrumentation scaling, data logging, and graphing for plotting and managing performance tests.

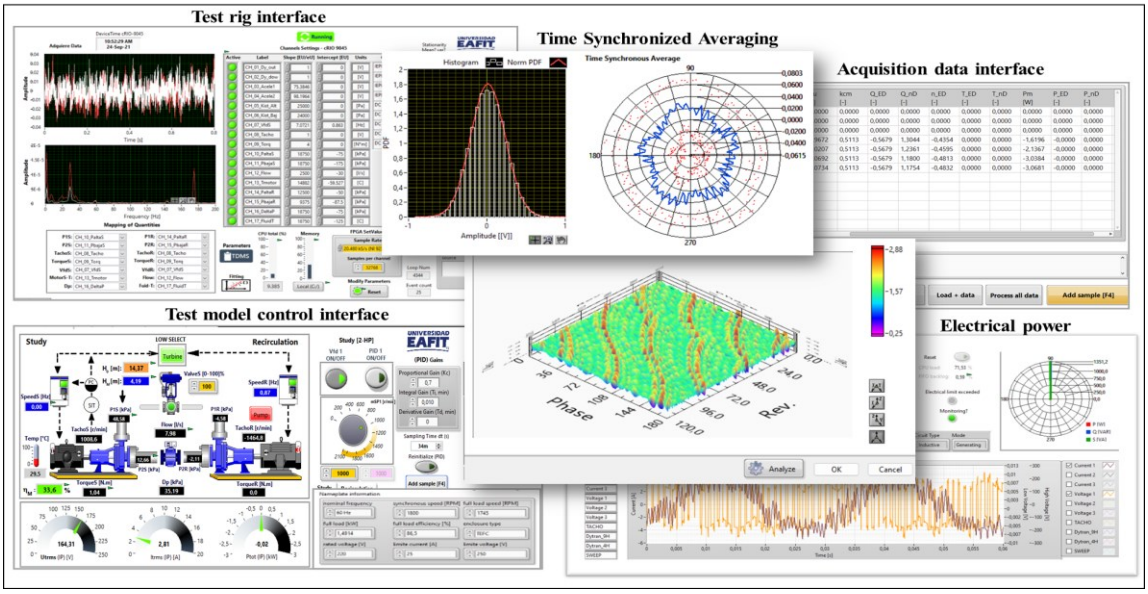

Figure 7. Human-machine interface for the monitoring of hydromechanical, dynamic, and electrical parameters of the turbomachine.

The development of these sequence models allowed measurements with simultaneous sampling rates, up to 102.4 kS/s for dynamic signals and up to 50 kS/s for electrical power signals (configurable by the user depending on the stability of the operating condition). In addition, the implemented sequencing model allows maintaining full control of the desired parameters during turbomachine characterization (test head, speed factor, discharge factor, among others) regardless of the assigned OP condition, thus allowing recording and displaying raw data of the hydromechanical and electrical signals, see Figure 8.

It also allows simultaneous monitoring of electrical power parameters related to the turbomachine motor, such as peak and root mean square (RMS) voltage and current, frequency, phase sequence, active power (P), apparent power (S), reactive power (Q), power factor (PF), phase angle shift and harmonics. The sine wave ripple shows the distortion produced by the nonlinear inductive load of the turbomachine's motor. Table 3 in Figure 8 (c) shows the parameters recorded close to the synchronous speed.

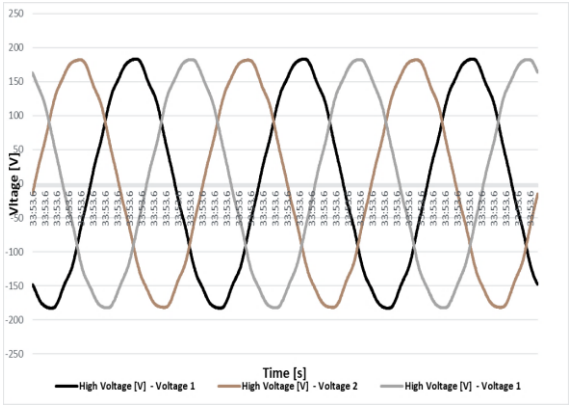

(**a**)

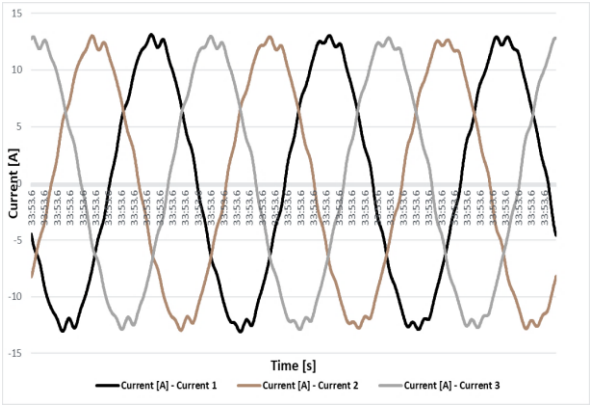

(**b**)

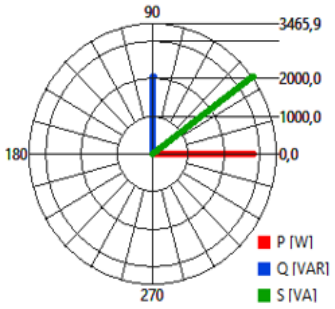

Table 3. Experimental results of electrical power parameters in pump mode.

Phase	Voltage peak [V]	Voltage rms [V]	Current rms [A]	Active [W]	Apparent [VA]	Reactive [VAr]	PF [-]
1	182.152	128.801	9.075	938.645	1168.946	696.692	0.803
2	181.395	128.266	8.949	928.353	1147.854	675.077	0.808
3	181.394	128.265	8.958	918.354	1149.1075	690.704	0.799

(**c**)

Figure 8. Electrical power signals upstream of the VFD. (a) Three-phase voltage waveform, (b) Three-phase current waveform. (c) Parameters were recorded close to the synchronous speed.

On the other hand, the data exchange system (RT Target) is the main software application and is used to manage high-speed data acquisition, processing, and transfer. In addition, it allows communication with the FPGA, management of the controller CPU load, and error monitoring of the digital platform. This application runs within the controller operating system to achieve the high sampling rates required for the acquisition of dynamic hydromechanical and electrical power signals.

The main processing step consists of two loops, high and low priority. The high-priority loop contains the functional blocks that perform the basic conditioning of the data, enable the synchronization of the acquisition rate of each controller, and set the buffer size for the data storage process. The low priority loop is deterministic (Control and Data Acquisition Loop) and runs at a lower speed than the high priority loop, its main function is to manage the network communication with the HMI through the SVEs and to control the Finite State Machine (FEM) developed at a software level.

Finally, the signal acquisition (FPGA) is the code developed on the FPGA embedded chip and includes high control-loop rates, determinism, and parallelism for the execution of multiple program routines. The compilation and implementation were developed in a hardware description language (HDL) code from the LabVIEW VIs module developed at the software level. In addition, tests performed during the measurement test were carried out with controlled loop rate timing to facilitate calculations and reduce FPGA memory consumption, achieving a guaranteed scan rate of 40µs for dynamic signals, using a 40MHz clock.

3.2 Characterization of the Turbomachine

To highlight the main functionalities and capabilities of the digital platform, the characterization in four quadrants of a reversible turbomachine is proposed. Considering a centrifugal pump can be characterized both as a pump and a turbine. Although different characteristic terms are available, the dimensionless terms of discharge and speed factors (Q_{ED}-n_{ED}) are chosen, as suggested by IEC-60193.

Operating points (OPs) were obtained by varying and controlling the speed of the rotor and the flow rate of the turbomachine. Between each operating point, the speed steps were varied every 50 rpm until the desired speed was reached and the corresponding flow rate was varied from 0.1 to 2 l/s respectively. The turbomachine was working at each point for about 5 minutes to have stable conditions.

During the performance tests, the entire operating range of interest of the turbomachine was covered, including stable and unstable operating points. In addition, at each operating point, dynamic signals were recorded at a sampling rate of 20,480 kS/s and the electrical power signals at 50 kS/s. Each DTMS file has a record data length of 20 blocks (packages) of 16,384 (2^{14}) samples per channel, for a total of 327,680 records stored for each variable per file.

The characteristic curve was plotted with 127 operating points covering the four quadrants of the turbomachine, over a speed range of 400 to 2000 rpm for pump and turbine mode. A more convenient way to construct the curve is to divide the test range into segments. Figure 9 illustrates some of the operating parameters of the turbomachine under study and the result of the four-quadrant characteristic curve developed in real-time, during the experimental tests.

In the screenshot, other quantities are obtained simultaneously, and that allows the position of the machine in the desired OP and make decisions as required. Some of them are static pressures (high and low), discharge, total dynamic head, NPSH, torque, etc.

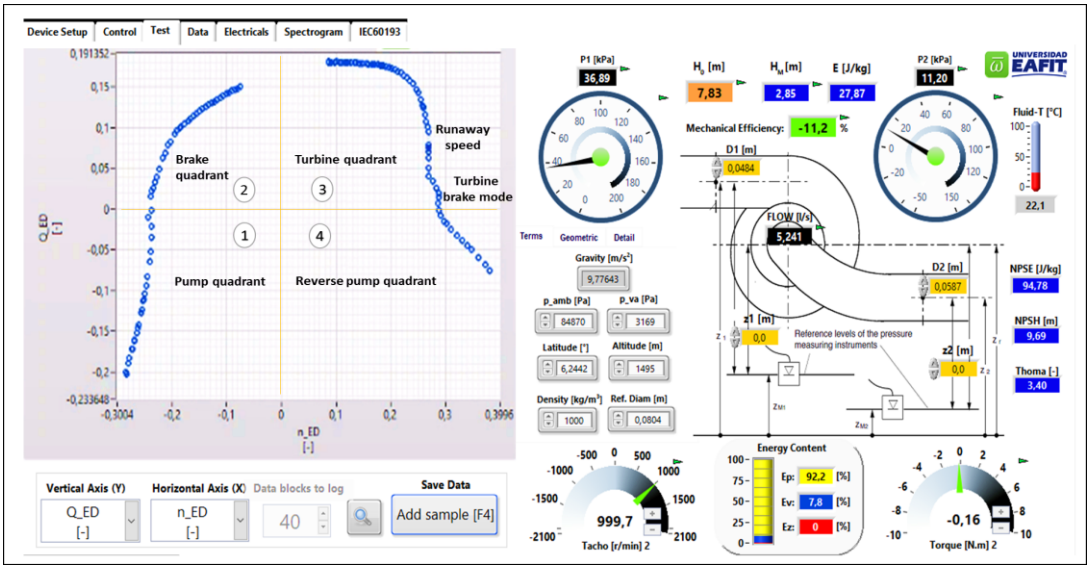

Figure 9. Graphical presentation of the results - 2 D Data plot interface developed during the turbomachine performance test.

The pump mode is characterized by negative discharge and negative rotational speed (see operating quadrant 1). This point represents the normal operating mode of the pump. The pump brake mode is characterized by a negative direction of rotation but a positive direction of discharge (see operating quadrant 2). This mode is transient and occurs in case of load rejection in pumping mode. The turbine mode has a positive discharge direction and rotational speed, and positive torque is supplied to the machine shaft (see operating quadrant 3). This point represents the normal operating mode of the turbine. The reverse rotation pump mode is characterized by a positive direction of rotational speed. However, the direction of discharge is negative (see operating quadrant 4). This mode can only be reached in transient conditions.

Runaway is a particular case, in which the torque is zero and corresponds to the turbine runaway (see operating quadrant 3). It occurs when the runaway speed is equal to the synchronous rotational speed of the machine. The turbine brake mode is a special case that has a positive discharge direction and rotational speed, but a negative torque (see operating quadrant 3). This mode occurs when the turbine is in run-in mode and the discharge decreases due to unstable phenomena or due to the closure of the guide vanes, head damper, or inlet damper during load rejection, i.e., under transient conditions.

3.3 Characteristic Curves

Although this work focuses on the four-quadrant characteristic curve, the platform also allows plotting the performance or behavior of the turbomachine for different tests or experimental tests. Some of the characteristic curves that can be constructed are the (Q-H) curve, the efficiency curve, the net positive suction

head (NPSH) curve, and some dimensionless curves established in IEC-60193 [27]. To construct such a curve, it is necessary to have a constant head, i.e., the head of a reservoir must be simulated in the laboratory, which implies that the available specific hydraulic energy E (or hydraulic head H) must remain constant. This is equivalent to keeping the dynamic pumping head at a fixed value. Thanks to the configuration of the test rig and the digital platform developed, it was possible to achieve this condition. Also, the specific energy was estimated in real-time from Bernoulli's equation. For the calculation of this equation, the instruments were installed as indicated in section 2.4 "Measuring Equipment".

Using other computational tools, the dimensionless curves of flow, torque, and power as a function of rotational speed are presented in Figure 10. The graphs were produced with the 127 TDMS files for the (n_{ED}-Q_{ED}), (n_{ED}-T_{ED}) and (n_{ED}-P_{ED}), coordinate systems. It should be noted that the four-quadrant characteristic curve (a) is equivalent to those produced in real-time during experimental tests with the TurboLogger software. In the case of the n_{ED}-T_{ED} and n_{ED}-P_{ED}, curves, their quadrants do not correspond directly to the quadrants of the n_{ED}-Q_{ED} characteristic (see Figure 10b). These curves were performed with a mean H of 4.21 mWC, a standard deviation of 0.06 mWC, and available E of 41.18 J/kg, with a standard deviation of 0.54 J/kg. With this information, the BEP in turbine mode was found to be at $n_{ED} = 0.168$, $Q_{ED} = 0.171$, giving a maximum efficiency of 41.6%.

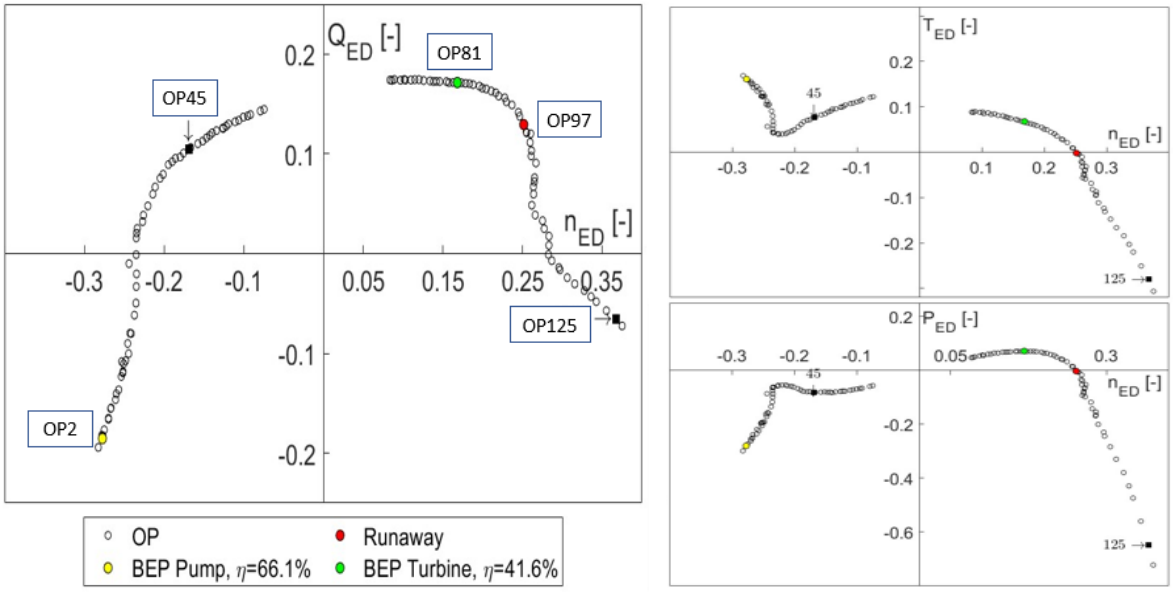

(**a**) (**b**)

Figure 10. Visualization of the characteristic curves of the turbomachine under study in the post-processing stage. (a) (n_{ED}-Q_{ED}) characteristic is properly called the four-quadrant curve. (b) curve (n_{ED}-T_{ED}) and curve (n_{ED}-P_{ED}).

The focus is on five specific OPs, where Table 4 shows the values of speed, flow, torque, and power factors recorded during the experimental tests, for the maximum efficiency points in pump mode and maximum efficiency in turbine mode, as well as the record of three specific out-of-design operating points, respectively. The first, OP2 corresponds to the BEP in pump mode. The second to OP45 is in the second quadrant and is the (Pump-Brake) mode. The third operating point corresponds to O81, which is the BEP in turbine mode, located in the third quadrant, in both quadrants are present spectral components related to dynamic fluctuations and pressure oscillations, possibly induced by hydrodynamic phenomena. The fourth, OP97, (Runaway), starts at the rotation stop where the no-load velocity condition occurs, i.e. ($Q_{ED} = 0$). The last point of interest is OP125 (Reverse pump), located in the fourth quadrant, where the highest vibration levels were expected to be detected.

Table 4. Selected operating points of the characteristic curves for the analysis.

Quadrant	Operating point	$n_{1,2}$[rpm]	$n_{ED}[-]$	$Q_{ED}[-]$	$T_{ED}[-]$	$P_{ED}[-]$
1	OP2: BEP Pump	-1348.43	-0.277	-0.185	0.161	-0.280
2	OP45: Pump-brake	-798.43	-0.168	0.104	0.076	-0.081
3	OP81: BEP Turbine	798.43	0.168	0.171	0.067	0.071
3	OP97: Runaway	1200	0.251	0.129	-0.002	-0.003
4	OP125: Reverse pump	1750	0.367	-0.065	-0.280	-0.648

3.4 Pressure Fluctuation and Accelerations

The synchronized recording between the stochastic signals associated with Group (b) "Dynamic sensors" with the speed signal of the tachometer or encoder, is another of the main advantages of the digital platform since this method allows to study and analyze at the same instant of time the behavior of the hydromechanical, dynamic and electrical power signals, produced by the instabilities of the flow. Thus, it is possible to analyze what happens in each revolution of the turbomachine and compare its behavior with other variables at out-of-design operating points, i.e., to carry out technical diagnostics. In this way, it is possible to observe and identify how a change in speed, flow rate, or operating regime affects especially pressure fluctuation or vibrations. However, it should be noted that the technical diagnostics of the turbomachine under study is beyond the scope of this article.

Another important aspect to consider is the amplitudes of the dynamic signals since they indicate high pressure variations or vibrations, which are normally expected to occur at deep part load, part load, high part load, and full load regime. With the database recorded during the experimental tests and using computational tools, the dynamic signals recorded are presented below, especially during the operation of the turbomachine in its BEP for turbine mode and in two off-design OPs where instabilities occur.

For this purpose, time, and frequency domain analysis methods, such as TSA and power spectra, were used to present the spectral components related to the hydrodynamic oscillations induced by the Blade Pass Frequency (BPF) of the turbomachine under study. Spectral analysis was also used to identify the sub-synchronous components that could be related to some of the hydrodynamic phenomena. With the signals recorded from the dynamic pressure fluctuation sensors DYT1 and acceleration sensors AC1 installed on the turbomachine's casing, spectral analysis has been performed focusing especially on three operating points (OP45, OP81, and OP125).

In the time domains, the pressure fluctuation signals are normalized by equation (1) according to the suggestion of the IEC-60193 [27].

$$\tilde{p}_E = \frac{p-\bar{p}}{\rho E} \tag{1}$$

Where $\tilde{p}_E$ is the pressure fluctuation coefficient, (p) is the instantaneous pressure N/m^2, $\bar{p}$ is the time-averaged pressure N/m^2. The pressure fluctuation amplitudes are made dimensionless by the representative pressure ρE of the specific hydraulic energy of the test.

In the frequency domains, for the analyses of pressure fluctuations and acceleration signals, the frequency spectrum was normalized. The frequencies were represented as a dimensionless coefficient f_n, defined by equation (2), established in IEC-60193 [27]. Power spectrum analysis was based on the Fast Fourier Transform (FFT) of pressure and vibration signals. The frequency band from 0 to 2.5 times the rotation speed of the machine was regarded, i.e.,$0 \leq f_n \leq 2.5$ [26].

$$f_n = \frac{f}{n} \tag{2}$$

Where the values of the pressure fluctuation frequency are made non-dimensional as a function of the impeller rotation frequency component f and the impeller rotation speed n.

To visualize the pressure fluctuations, an FFT was performed for the DYT1 signals recorded at each of the OPs. For instance, note that the impeller rotation speed at OP81 is 798.43 rpm, which indicates that the impeller rotation frequency component f is 13.31Hz, leading to a BPF of 79.84 Hz.

Therefore, there is a blade passing spectral component of 6x; this is because the turbomachine under study has a six-bladed centrifugal impeller, and they pass six times at a particular point during each revolution. Thus, to detect phenomena that produce pressure fluctuation components and that have a fixed relationship with the shaft rotational speed, the frequency is expressed as a function of the machine impeller rotational speed. This spectral analysis makes it possible to detect both synchronous and asynchronous components, focusing on their characteristics (amplitude and frequency). On the other hand, the sub-synchronous band (up to 1x) in some operating regimes is dominated by disturbances and instabilities that could be related to hydrodynamic phenomena with sub-synchronous components.

After performing an analysis of the dynamic pressure and acceleration signals captured with the integrated digital platform described above, it was possible to perform a more detailed study and analysis of the behavior of the pressure fluctuations and accelerations produced within the turbomachine, where dominant spectral components of 1x, 6x, present in all operating modes were evidenced. The 1x component represents the shaft frequency and the 6x component is the BPF of the turbomachine under study. Figure 12 below shows the frequency spectrum of the three OPs, found as a function of the f_n and $\tilde{p}_E$, from which we can conclude that the components related to the pressure fluctuations induced by the BPF and its harmonics were the main dominant frequencies of the turbomachine under study. Moreover, the different charts exhibited different pressure pulsation characteristics. The polar representation of the TSA for the three operating points is also presented, where the red lines correspond to TSA±1 (σ).

Figure 11 shows the patterns related to the power spectra for the three OPs, where the light blue line represents the behavior of the turbomachine in OP45, the green line represents the behavior in its BEP, OP81, furthermore, the red line indicates the behavior in Runaway. Finally, the blue line shows the behavior of the turbomachine under study in OP125, that is, in the fourth quadrant, reverse pump mode, where the component with the largest pressure fluctuation amplitude is presented. In addition, for this operating point, slight pressure peaks in the sub-synchronous band (up to 1x) can be observed.

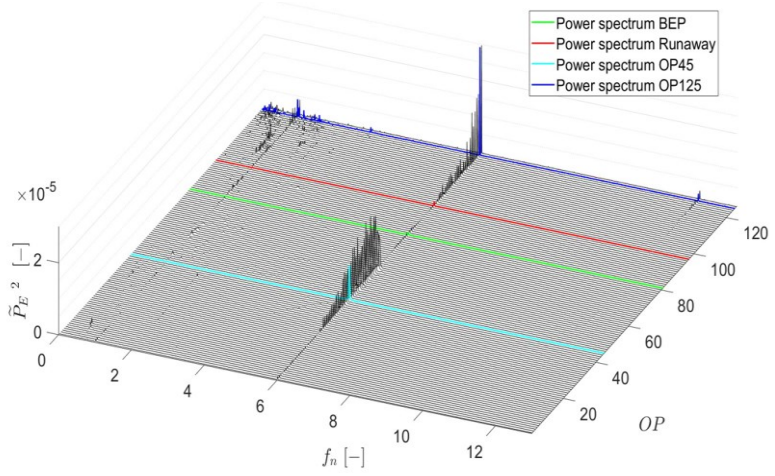

Figure 11. Frequency spectrum as a function of pressure fluctuations, frequency, and operating points, signals obtained from the pressure sensor DYT1 for each of the points of interest.

As shown in Figure 12, while OP45 recorded the lowest level of pressure amplitudes and presents some sub-synchronous components, OP81, and its vicinity showed a representative increase in pressure amplitudes that could also be related to fluid instabilities and hydrodynamic phenomena. Considering that OP45 and the vicinity of the BEP are in an operating regime at off-design conditions of the turbomachine, it is expected to detect this type of behavior. Also, OP125 presented the highest level of pressure pulsation amplitudes. However, it can be appreciated that some of the pressure pulsation frequencies present within the turbomachine in each of the OPs are related to the shaft and impeller rotation frequency, where dominant spectral components of 1x, 6x, and 12x were evidenced.

However, for the same OPs, high vibration peaks appear with frequencies of 18x, 26x, and 28x, which could also be related to harmonics generated by unstable and transient behaviors associated especially by their frequency and amplitude to hydrodynamic phenomena, perhaps induced by load variations or electrical aspects since mechanical imbalances and misalignments are related to low frequencies (1x, 2x) [33]. In Figure 12, there are also other low-frequency components shown in the frequency domain. However, some of their amplitudes are rather limited.

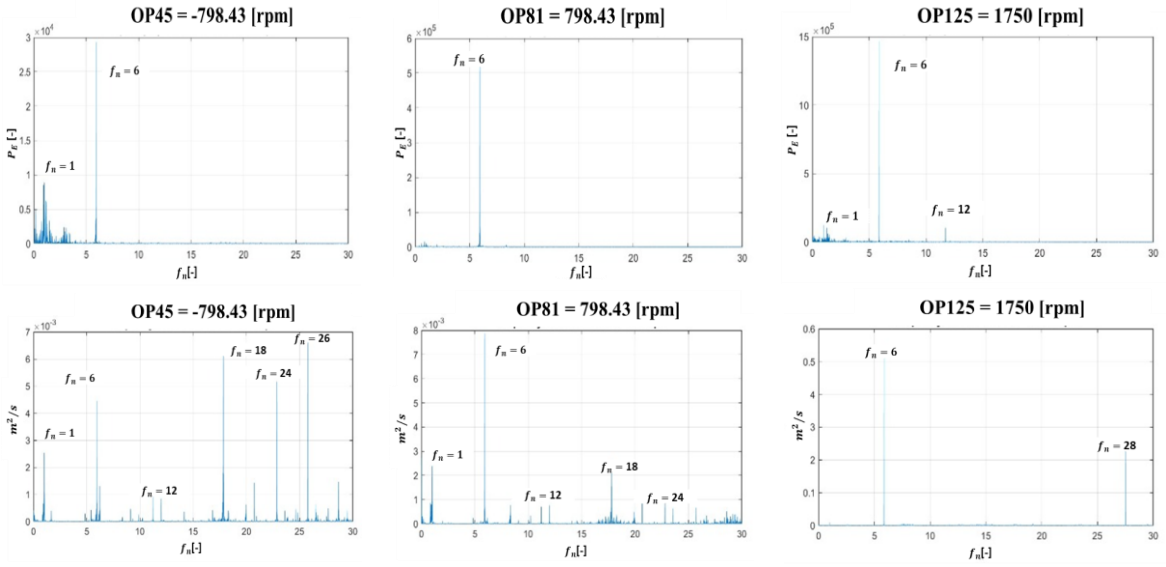

(**a**) (**b**) (**c**)

Figure 12. Frequency spectrum for the pressure fluctuation and vibration signals at the 3 selected points of the four-quadrant characteristic curve. (a) shows point (OP45) Pump-Brake, dominant frequency f_n=1x,6x,12x,18x,24x and 26x. (b) show the BEP (OP81), dominant frequency f_n=1x,6x,12x,18x and 24x. (c) show the point (OP125) Reverse pump, dominant frequency f_n= 1x,6x,12x and 28x.

Each segment of the chart in Figure 13 is called a rose petal and the number of petals corresponds to the 6 blades of the turbomachine impeller.

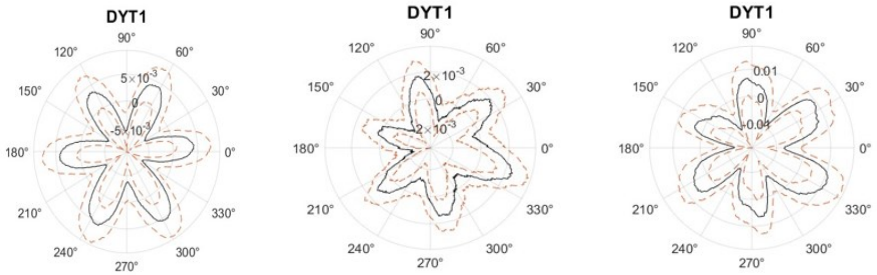

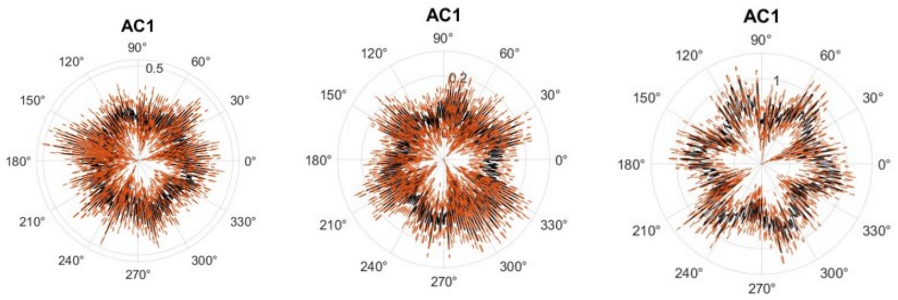

(**a**) (**b**) (**c**)

Figure 13. Time domain plot analysis (TSA) for 3 representative points of the characteristic curve (n_{ED}-Q_{ED}), measurement of pressure fluctuation and vibrations. (a) shows point (OP45) Pump-Brake. (b) shows point (OP81) BEP. (c) shows point (OP125) Reverse pump.

It can be seen in Figure 13a, that the TSA of OP45 shows that the pressure is well distributed around the circumference, suggesting that possible hydrodynamic phenomena present at this operating point do not affect the performance of the turbomachine. The TSA at OP81 shows that Figure 13b, despite being the point of highest performance, the turbomachine exhibits instabilities possibly produced or associated by flow disturbances that could be the result of rotodynamic forces, or others that are transferred from the shaft to the rotor, induced by flow oscillations, which may occur at the sub-synchronous level [26], [33].

However, there is no certainty since the evidence gathered in the research is not sufficient to explain these phenomena, since the analysis of these behaviors is part of the technical diagnostic that is beyond the scope of this article. Concerning OP125 as shown in Figure 13c, the TSA presents some deformations, since the highest-pressure pulsations and vibrations of the turbomachine occur at the (fourth quadrant). Figure 14a, shows the experimental test rig setup and the photograph of one of the recorded phenomena.

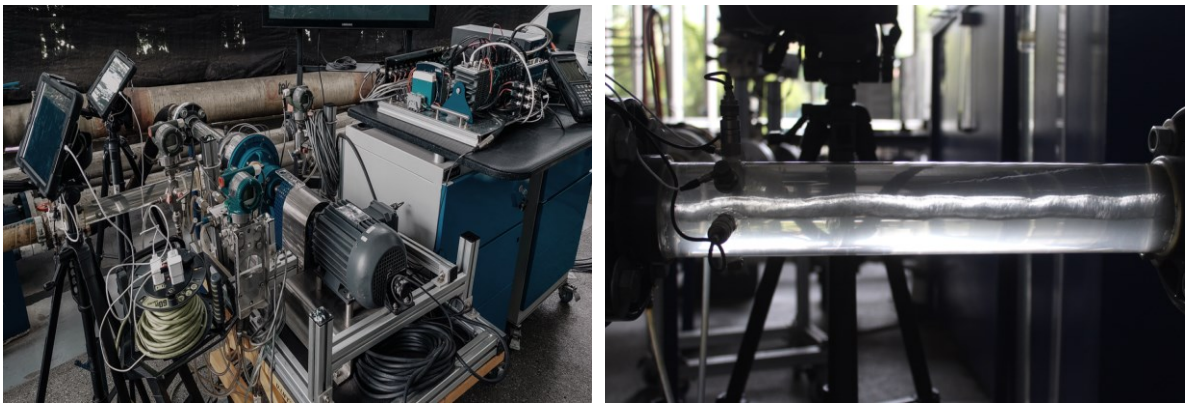

(**a**) (**b**)

Figure 14. Recording of complex hydrodynamic phenomena. (a) Experimental test rig setup (b) Visualization during the experimental test of a vortex rope.

During experimental tests, one of the flow patterns observed in some OPs in the pump-brake mode (second quadrant) was the vortex rope type, see Figure 14b. This phenomenon is generated in the draft tube of turbomachines and consists of a vortex with a low-pressure core where cavitation occurs. In the case of the turbomachine under study, it was observed in the acrylic tube of the low-pressure reference section. Therefore, from the analyses carried out, the results, and the characteristics of the dynamic signals, it is concluded that the main pressure pulsations and accelerations recorded with the TurboLogger software during the experimental tests are related to the periodic effect of the BPF and/or instabilities related to some of the hydrodynamic phenomena that occur in the reversible turbomachines.

4. Conclusions

The TurboLogger autonomously followed the detailed characterization process of a PaT through its four-quadrant characteristic curve and revealed complex hydraulic phenomena manifested at some of the observed operating points. It also allowed to characterize the electric fluid of the induction motor of the studied machine, which is an advantage that will allow a future study of the energy quality generated in its BEP. Also, this digital platform was developed to integrate the functions of measurement, data acquisition, and real-time monitoring of deterministic and stochastic signals with high sampling rates and high resolution, thus ensuring continuous and multichannel measurement.

The TurboLogger processes and handles both stochastic and deterministic, hydraulic, mechanical, and electrical variables, which allowed examining the behavior of each of the signals in the time, frequency, and time-frequency domains. In addition, the TDMS format adopted allowed the platform to easily exchange information with other programming environments or information processing systems, thus avoiding the costly and time-consuming design and maintenance of architectures and databases. Its files are binary and efficiently structured for high-speed writing.

Deterministic, and stochastic signals were classified into four groups as follows: Group (a) for all hydromechanical signals used for machine characterization. Group (b) exclusively for dynamic signals used to study hydrodynamic phenomena. Group (c) integrates the electrical power signals used to analyze the phenomena produced by power supply fluctuations, and Group (d) is assigned to the control signals. This classification allowed the specific selection of the hardware components and the development of the software processing structure.

One of the main advantages of the methodology implemented in the digital platform focused on the Common Data Environment (CDE), which allowed all researchers to work from the same programming model, ensuring the most updated version of the software, the basic configuration parameters, and the same database. Thus, the platform environment became a central data repository for all research project documentation, facilitating the management of the large volume of information generated during experimental testing. The exchange of information with other expert programming languages was also validated by properly exporting and processing the records acquired with the TurboLogger.

The information presented in this work is important for the monitoring, characterization, study, and research of hydrodynamic phenomena, specifically reversible hydraulic turbomachines. Therefore, from the analyses carried out, the results, and the characteristics of the dynamic signals, it is concluded that the main pressure pulsations and accelerations recorded with the TurboLogger software during the experimental tests are related to the periodic effect of the BPF and/or instabilities related to some of the hydrodynamic phenomena that occur in the reversible turbomachines. Even the instrumentation and methods considered in this work allow obtaining evidence to detect sub-synchronous hydrodynamic phenomena.

The turbomachine under study presents multiple hydrodynamic rotational phenomena that deserve to be identified and studied, many of which were not analyzed and characterized since the technical diagnosis of the turbomachine studied is beyond the scope of this article. Nevertheless, the research gathered evidence showing that the TurboLogger software, although oriented to a small PaT, can be adapted to large-scale machines and even to other types of turbomachines.

5. Declaration of competing interest

I declare that I have no significant competing interests, including financial or non-financial, professional, or personal interests interfering with the full and objective presentation of the work described in this manuscript.

6. Acknowledgments

The author would like to thank EAFIT University and the Hydraulics Laboratory of EAFIT University for the unconditional technical support provided for the development of this work.

7. References

[1] "Hydropower Program | Department of Energy." https://www.energy.gov/eere/water/hydropower-program (accessed Aug. 05, 2022).

[2] "IRENA – International Renewable Energy Agency." https://www.irena.org/ (accessed Jul. 20, 2022).

[3] "Renewables - Fuels & Technologies - IEA." https://www.iea.org/fuels-and-technologies/renewables (accessed Jul. 18, 2022).

[4] C. P. Jawahar and P. A. Michael, "A review on turbines for micro hydro power plant," *Renewable and Sustainable Energy Reviews*, vol. 72. Elsevier Ltd, pp. 882–887, 2017. doi: 10.1016/j.rser.2017.01.133.

[5] I. M. Hossain, S. M. Ferdous, S. Salehin, A. M. Saleque, and T. Jamal, "Pump-as-turbine (PAT) for small scale power generation: A comparative analysis," *Proceedings of 2014 3rd International Conference on the Developments in Renewable Energy Technology, ICDRET 2014*, no. February 2015, 2014, doi: 10.1109/icdret.2014.6861698.

[6] "MICRO AND PICO HYDRO - British Hydro Association." https://www.british-hydro.org/micro-hydro/ (accessed Aug. 03, 2022).

[7] A. Morabito and P. Hendrick, "Pump as turbine applied to micro energy storage and smart water grids: A case study," *Appl Energy*, vol. 241, pp. 567–579, May 2019, doi: 10.1016/j.apenergy.2019.03.018.

[8] S. v. Jain and R. N. Patel, "Investigations on pump running in turbine mode: A review of the state-of-the-art," *Renewable and Sustainable Energy Reviews*, vol. 30. Elsevier Ltd, pp. 841–868, 2014. doi: 10.1016/j.rser.2013.11.030.

[9] V. Hasmatuchi, F. Botero, S. Gabathuler, and C. Münch-Alligné, "Design and control of a new hydraulic test rig for small-power turbomachines," *Hydro 2014*, no. Four, pp. 54–60, 2014.

[10] "Research – PTMH - EPFL." https://www.epfl.ch/research/facilities/hydraulic-machines-platform/ptmh/research/ (accessed Aug. 12, 2022).

[11] "On the Dynamic Measurements of Hydraulic Characteristics".

[12] M. Arriaga, "Pump as turbine - A pico-hydro alternative in Lao People's Democratic Republic," *Renew Energy*, vol. 35, no. 5, pp. 1109–1115, 2010, doi: 10.1016/j.renene.2009.08.022.

[13] A. H. Elbatran, O. B. Yaakob, Y. M. Ahmed, and H. M. Shabara, "Operation, performance and economic analysis of low head micro-hydropower turbines for rural and remote areas: A review," *Renewable and Sustainable Energy Reviews*, vol. 43. Elsevier Ltd, pp. 40–50, 2015. doi: 10.1016/j.rser.2014.11.045.

[14] M. Binama, W. T. Su, X. bin Li, F. C. Li, X. Z. Wei, and S. An, "Investigation on pump as turbine (PAT) technical aspects for micro hydropower schemes: A state-of-the-art review," *Renewable and Sustainable Energy Reviews*, vol. 79, no. February, pp. 148–179, 2017, doi: 10.1016/j.rser.2017.04.071.

[15] J. C. Alberizzi, M. Renzi, A. Nigro, and M. Rossi, "Study of a Pump-as-Turbine (PaT) speed control for a Water Distribution Network (WDN) in South-Tyrol subjected to high variable water flow rates," in *Energy Procedia*, 2018, vol. 148, pp. 226–233. doi: 10.1016/j.egypro.2018.08.072.

[16] G. M. Lima, E. L. Junior, and B. M. Brentan, "Selection of Pumps as Turbines Substituting Pressure Reducing Valves," *Procedia Eng*, vol. 186, pp. 676–683, 2017, doi: 10.1016/j.proeng.2017.06.249.

[17] M. Stefanizzi, T. Capurso, G. Balacco, M. Binetti, S. M. Camporeale, and M. Torresi, "Selection, control and techno-economic feasibility of Pumps as Turbines in Water Distribution Networks," *Renew Energy*, vol. 162, pp. 1292–1306, Dec. 2020, doi: 10.1016/j.renene.2020.08.108.

[18] A. Morabito and P. Hendrick, "Pump as turbine applied to micro energy storage and smart water grids: A case study," *Appl Energy*, vol. 241, no. August 2018, pp. 567–579, 2019, doi: 10.1016/j.apenergy.2019.03.018.

[19] S. Barbarelli, M. Amelio, G. Florio, and N. M. Scornaienchi, "Procedure Selecting Pumps Running as Turbines in Micro Hydro Plants," *Energy Procedia*, vol. 126, pp. 549–556, 2017, doi: 10.1016/j.egypro.2017.08.282.

[20] T. Lin, Z. Zhu, X. Li, J. Li, and Y. Lin, "Theoretical, experimental, and numerical methods to predict the best efficiency point of centrifugal pump as turbine," *Renew Energy*, vol. 168, pp. 31–44, May 2021, doi: 10.1016/j.renene.2020.12.040.

[21] M. Rossi, A. Nigro, and M. Renzi, "A predicting model of PaTs' performance in off-design operating conditions," in *Energy Procedia*, 2019, vol. 158, pp. 123–128. doi: 10.1016/j.egypro.2019.01.056.

[22] Y. Sun, Z. Zuo, S. Liu, J. Liu, and Y. Wu, "Distribution of pressure fluctuations in a prototype pump turbine at pump mode," *Advances in Mechanical Engineering*, vol. 2014, 2014, doi: 10.1155/2014/923937.

[23] U. Eafit, "CENTRÍFUGA EN RELACIÓN CON SU CURVA CARACTERÍSTICA," 2016.

[24] R. T. Knapp, “Complete Characteristics of Centrifugal Pumps and Their Use in the Prediction of Transient Behavior,” *Transactions of the A.S.M.E.*, pp. 683–689, 1937.
[25] H. Amblard, G. Borciani, P. Guiton, P. Henry, G. Martin, and R. Thalmann, “Behaviour of Francis turbines and pump turbines at partial flow rate.,” *Houille Blanche*, vol. 6368, no. 5, 1985, pp. 435–440, 1985, doi: 10.1051/lhb/1985031.
[26] H. D. Bolaños and F. Botero, “Four-quadrant characterization of hydrodynamic phenomena in a low specific speed centrifugal pump,” *Ingenieria y Universidad*, vol. 25, 2021, doi: 10.11144/Javeriana.iued25.fchp.
[27] International Electrotechnical Commission, *International Standard IEC 60193*, 3.0., vol. 1, no. June. IEC, 2019.
[28] “The NI TDMS File Format - NI.” https://www.ni.com/en-us/support/documentation/supplemental/06/the-ni-tdms-file-format.html (accessed Sep. 12, 2022).
[29] D. Tobón, “Estudio numérico y experimental de fenómenos hidrodinámicos que ocurren en bombas centrífugas como turbinas,” Universidad EAFIT, Medellín, 2016.
[30] H. Bolaños, “Fenómenos hidrodinámicos periódicos en una bomba centrífuga de baja velocidad específica,” Universidad EAFIT, Medellín, 2018. Accessed: Jul. 17, 2022. [Online]. Available: https://repository.eafit.edu.co/handle/10784/12998
[31] D. Valentín, A. Presas, C. Valero, M. Egusquiza, and E. Egusquiza, “Detection of hydraulic phenomena in francis turbines with different sensors,” *Sensors (Switzerland)*, vol. 19, no. 18, Sep. 2019, doi: 10.3390/s19184053.
[32] Z. Zuo, S. Liu, Y. Sun, and Y. Wu, “Pressure fluctuations in the vaneless space of High-head pump-turbines - A review,” *Renewable and Sustainable Energy Reviews*, vol. 41. Elsevier Ltd, pp. 965–974, Jan. 01, 2015. doi: 10.1016/j.rser.2014.09.011.
[33] C. E. Brennen, “Hydrodynamics of pumps,” in *Hydrodynamics of Pumps*, vol. 9781107002371, Cambridge University Press, 2011, pp. 129–168. doi: 10.1017/CBO9780511976728.
[34] V. Hasmatuchi, M. Farhat, S. Roth, F. Botero, and F. Avellan, “Experimental evidence of rotating stall in a pump-turbine at off-design conditions in generating mode,” *Journal of Fluids Engineering, Transactions of the ASME*, vol. 133, no. 5, 2011, doi: 10.1115/1.4004088.
[35] F. Botero, V. Hasmatuchi, S. Roth, and M. Farhat, “Non-intrusive detection of rotating stall in pump-turbines,” *Mech Syst Signal Process*, vol. 48, no. 1–2, pp. 162–173, Oct. 2014, doi: 10.1016/j.ymssp.2014.03.007.
[36] G. Pumps, “Goulds pumps, G&L Series SSH,S & M-Group 316 Stainless Steel End Suction Pumps,” *World Pumps*. ITT Corporation, p. 36, 2006. doi: 10.1016/s0262-1762(00)80065-6.
[37] J. G. McCoy, Gilbert A.; Douglass, “Premium efficiency motor selection and application guide - A handbook for industry,” *Energy Efficiency & Renewable Energy*. p. 136, 2014.
[38] “CompactRIO Systems - NI.” https://www.ni.com/en-us/shop/compactrio.html (accessed Aug. 12, 2022).
[39] “CompactRIO Modules - NI.” https://www.ni.com/en-us/shop/compactrio/compactrio-modules.html (accessed Sep. 17, 2022).
[40] S. Alligné *et al.*, “Turbine mode start-up simulation of a FSFC variable speed pump-turbine prototype - Part I: 1D simulation,” in *IOP Conference Series: Earth and Environmental Science*, Jun. 2021, vol. 774, no. 1. doi: 10.1088/1755-1315/774/1/012052.
[41] “Using Shared Variables in Executables - NI.” https://www.ni.com/es-co/support/documentation/supplemental/07/using-shared-variables-in-executables.html (accessed Aug. 03, 2022).